Eur. Phys. J. B **29**, 51–59 (2002)
DOI: 10.1140/epjb/e2002-00261-3

THE EUROPEAN PHYSICAL JOURNAL B

The Al-Pd-Mn quasicrystalline approximant ξ'-phase revisited

N. Shramchenko[1,2] and F. Dénoyer[3,a]

[1] Laboratoire Léon Brillouin (CEA-CNRS), CEA Saclay, 91191 Gif-sur-Yvette cedex, France
[2] Laboratoire d'Étude des Microstructures (ONERA-CNRS), BP 72, 92320 Châtillon Cedex, France
[3] Laboratoire de Physique des Solides[b], bâtiment 510, Université Paris-Sud, 91405 Orsay Cedex, France

Received 11 April 2002 / Received in final form 24 June 2002
Published online 17 September 2002 –

Abstract. A detailed investigation of the Fourier space of several Al-Pd-Mn samples with composition Al-72.6 at. %, Pd-22.9 at. %, Mn-4.5 at. % is reported. In the phase diagram of the Al-Pd-Mn ternary alloy, this composition corresponds to the so-called ξ' phase which was described as an icosahedral quasicrystalline approximant. By re-examining the Fourier space by means of X-ray diffraction (powder patterns and single crystal precession patterns), complex structures in close relation with the ξ'-phase have been observed. These long-range order complex structures are described as resulting from a periodic perturbation of the ξ' structure along the c direction. Two states with periodicities $c_{\xi'}(3+\tau)$ and $c_{\xi'}(5+\tau)$ have been observed in this study (τ: golden mean). Structural models based on periodic arrangements of "defects" layers separating layers of ξ' phase are proposed. These two states are certainly intermediate states between the ξ' phase and the metastable decagonal quasicrystalline phase.

PACS. 61.44.Br Quasicrystal – 61.10.-i X-ray diffraction and scattering – 61.10Nz Single crystal and powder diffraction

1 Introduction

Since the discovery of quasicrystals and despite great efforts in the growth of large single quasicrystals and developments of more and more sophisticated atomic structure models in high dimensional spaces, the agreement between calculated and measured diffraction peak spectra is still far from being satisfactory. In this paper, we choose to study quasicrystalline approximants that are periodic structures having many features in common with their parent quasicrystalline structures.

In the rapidly solidified Al-Pd binary alloy, a crystalline Al_3Pd phase was reported as an *approximant of a decagonal* phase and a transformation from the *decagonal quasicrystal* to the Al_3Pd crystalline phase was observed in electron diffraction experiments [1]. This crystalline phase was defined as a quasicrystal approximant owing to its close structural orientational relationships with the decagonal quasicrystal. A few years later, Matsuo and Hiraga [2] could obtain a small single crystal of Al_3Pd for refining the structure (atomic arrangement) of this alloy. Combining atomic structure and high-resolution electron microscopy (HREM) images, they could characterize the structure as a periodic two-dimensional arrangement (in the (**a**, **c**) plane) of decagonal columns (radius of columns = 3.807 Å and periodicity $b = 16.59$ Å along the columns). Moreover, the rapid quenched Al_3Pd decagonal quasicrystal was studied by high-resolution electron microscopy and the images show a quasiperiodic two-dimensional arrangement of the same decagonal columns [3].

Not long after, a rapid quenched *decagonal* phase similar to the 2D decagonal quasicrystal Al_3Pd with the same periodicity along the columns could be observed in the Al-Pd-Mn ternary alloy in the Pd rich ($\simeq$ 25at. %) and Mn poor ($<$ 5at. %) region [4]. More recently, large single crystals ($\simeq 1\text{cm}^3$) of a *periodic orthorhombic phase called the ξ' phase* were obtained by several groups [5–7]. The crystal structure of this ξ' phase was refined from X-ray data collections [5,8]. In spite of different attributed space group ($Pn2_1a$ and $Pnma$), the structures of Al_3Pd and ξ' (composition $Al_{73.5}\ Pd_{22.4}\ Mn_{4.1}$) were found very similar with almost equal lattice parameters:

$$a_{\xi'} = 23.541 \text{ Å} \quad a_{Al_3Pd} = 23.36 \text{ Å}$$

$$b_{\xi'} = 16.566 \text{ Å} \quad b_{Al_3Pd} = 16.59 \text{ Å}$$

$$c_{\xi'} = 12.339 \text{ Å} \quad c_{Al_3Pd} = 12.32 \text{ Å}.$$

According to transmission electron microscopy results, structural orientational relationships (epitaxy) were found between the ξ' *phase and the Al-Pd-Mn icosahedral quasicrystal phase* [8,9]. Consequently, Klein *et al.* have

[a] e-mail: denoyer@lps.u-psud.fr
[b] (UMR 8502)

proposed to describe the ξ' structure as an *icosahedral quasicrystalline approximant*. It is worth mentioning that the icosahedral phase is stable in a small composition region around the ideal composition $Al_{69.9}Pd_{21.7}Al_{8.4}$.

A theoretical method to describe approximants as periodic crystals derived from quasicrystals consists in applying the "perpendicular shear method" to the high dimensional space of a quasicrystal. This method was first proposed by Jaric and Qiu [10] and then later developed by several others authors [11–13].

By applying this method to the Fourier space of a quasicrystal, the Fourier space of the rational approximant (position of periodic Bragg peaks and their approximative intensities) is easily obtained. Such studies for different compounds were performed as well for icosahedral as for decagonal approximants [14–18].

Attempts at applying this shear method to the icosahedral Al-Pd-Mn quasicrystal in order to obtain the theoretical ξ' phase, have been published [8,9,19]. However the authors have experienced several difficulties. The first is the absence of group-subgroup relation for the transformation from the icosahedral quasicrystalline phase to the orthorhombic ξ' approximant. The second is the absence of a selective point in the 6D cell of the icosahedral quasicrystal giving the **b** basic vector of the ξ' approximant (the modulus of the 6D vector corresponding to the existing node in the 6D cell of the icosahedral quasicrystal being two times larger). With such a 6D vector, a superstructure two along the b direction is expected. The questions are as follows: is the orthorhombic symmetry the right symmetry of the ξ' phase and does a $2b$ superstructure exist or not? In the case of negative answers, another explanation has to be found. For example, owing to the similarities between Al_3Pd and ξ' structures, a description in terms of a *decagonal quasicrystal approximant* could be also considered and although the decagonal phase with a 16 Å periodicity was not yet found as a stable but metastable decagonal quasicrystal in the Al-Pd-Mn alloy, it would be interesting to apply the shear technique to this decagonal quasicrystal [20].

The Al-Pd-Mn system is one of the few systems for which large single grains of icosahedral quasicrystals and approximant crystals are available. It is an ideal system for the comparison of structural and physical properties between approximant periodic crystal and non-periodic quasicrystal. It is therefore important to perform a *complete Fourier space* analysis in exploring the Fourier space by means of X-ray diffraction technique in order to answer these questions. Such a study is the subject of this current paper.

2 Sample description

Samples of Al-Pd-Mn with composition around Al-72.6 at.%, Pd-22.9 at.%, Mn-4.5 at.% corresponding to a nominal composition of the ξ' phase were elaborated at the Institut für Festkörperforschung in Jülich, using Bridgman crystal growth method. Samples called 1, 2 and 3 have volumes estimated at $V_1 = 1.3$ cm^3, $V_2 = 1.2$ cm^3 and $V_3 = 1.5$ cm^3 and their density measured by picnometric method is equal to 4.89 g/cm^3. In order to identify the single grain parts of these samples, γ-ray diffraction (collaboration with P. Bastie, ILL, Grenoble) were performed. The rocking curves were measured around the a, b and c directions for the three samples. Samples 1 and 2 have shown the same type of curves: several grains distributed on nearly 3 degrees with a particularity for the curve measured around the b direction. This particularity consists of a "rough plateau", the better the quality of the crystal around the a and c direction, the less the "rugosity" of the "plateau" was. Such a particularity was not observed on the sample 3. Single grains K1, K2 with typical dimensions $3 \times 3 \times 3$ mm^3 were taken from samples 1 and 2 respectively and their mosaic spread were tested again.

3 X-ray diffraction experiments

3.1 X-ray powder diffraction study

Up to now, no powder X-ray diffraction patterns have been presented in the literature for the ξ' phase. Powder diffraction experiments were carried out, on a diffractometer installed on the beamline W22 located on a wiggler of the Laboratoire pour l'Utilisation du Rayonnement Synchrotron (LURE, Orsay, France). Three powder samples were prepared from small pieces of samples 1, 2 and 3. Their powder diffraction patterns were obtained by $\theta - 2\theta$ scans using a wavelength $\lambda = 0.688$ Å. The diffracted intensities were also recorded on imaging plates, in order to check the spatial homogeneity of diffraction rings, *i.e.* the absence of texture effects.

The X-ray powder patterns are given in Figures 1a, 2a, 3a for the three samples. We proceeded in the following way in indexing our spectra: the X-ray powder diffraction pattern was first calculated from the published ξ' structure [5,8], then compared to our data. Surprisingly, their superpositions on measured spectra only give a good agreement for $(h\,k\,0)$ reflections, slight shifts of $(h\,k\,l)$ reflections with $\ell \neq 0$ being observed for the three powder samples.

The a and b lattice parameters have been deduced from $(h\,k\,0)$ reflections. Their values $a = 23.574$ Å and $b = 16.610$ Å of the powder sample 3 are found slightly larger than the values $a = 23.531$ Å and $b = 16.580$ Å of the powder samples 1 and 2. Indexing the peaks $(h\,k\,l)$ with $\ell \neq 0$ has required a strong increase of the c parameter value. It takes the values: $c = 57.120$ Å for the sample 3 and $c = 81.832$ Å for the samples 1 and 2. Selected parts (the more intense regions) of indexed diagrams together with intensities arising from their related ξ' diffraction peaks are shown in Figures 1b–d, 2b–d and 3b–d for the 1, 2 and 3 powder samples respectively. In this procedure, we have only considered the peaks of the ξ' structure having intensities $> 0.01\,I_1$, where I_1 is the intensity of the strongest peak of the ξ' structure.

By analysing some HREM images of references [8,21], we have been able to locally observe periodicity $c_{\xi'}(2+\tau)$

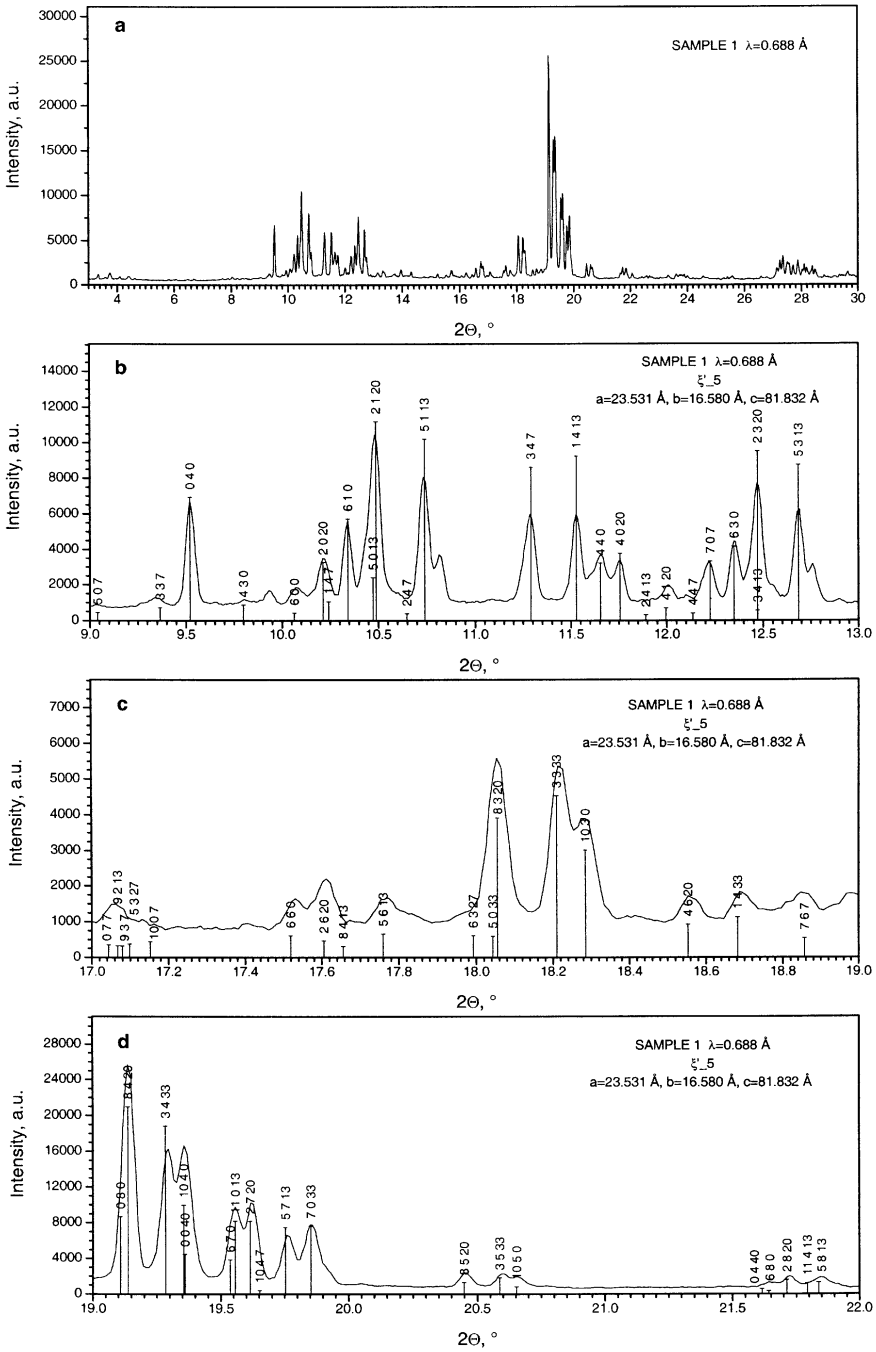

Fig. 1. X-ray powder diffraction pattern ($\theta - 2\theta$ scan, $\lambda = 0.688$ Å) of sample 1. $\theta - 2\theta$ scan is measured with a θ step equal to 0.005°. The lines drawn are lines connecting data points. (a) The whole spectrum. The indexed spectrum in the following regions: (b) $9° < \theta < 13°$, (c) $17° < \theta < 19°$ and (d) $19° < \theta < 22°$. The weak peak which appears at $2\theta = 9.935°$ can be attributed to the (0 1 20) reflection (calculated $2\theta = 9.936°$). It is not reported in (b) because it is arising from the (0 1 3) reflection of the ξ' structure (intensity = 0.004 I_1).

where τ is the golden mean. Regarding the c lattice parameters measured in our high resolution X-ray pattern, we can define $c = 57.120$ Å as $c_{\xi'}(3+\tau)$ and $c = 81.832$ Å as $c_{\xi'}(5+\tau)$. In the following these states will be called the ξ'_3 and the ξ'_5 state respectively.

These X-ray powder diffraction results indicate that none of studied powder samples has the ξ' structure [5,8] but their structures are very close to it. In fact, the height of diffraction lines that we have attributed to each $(h\,k\,l)$ measured peak (straight lines together with their indices in Figs. 1b–d, 2b–d and 3b–d) corresponds to the intensity that we have calculated from the published ξ' structure [5,8], providing we transform the indices $l = 0, 1, 2, 3, 5, 6$ of the ξ' phase into the indices $\ell = 0, 7, 13, 20, 33, 40$ of the ξ'_5 state (see Figs. 1b–d and 2b–d) or into the indices $\ell = 0, 5, 9, 14, 23, 28$ of ξ'_3 state

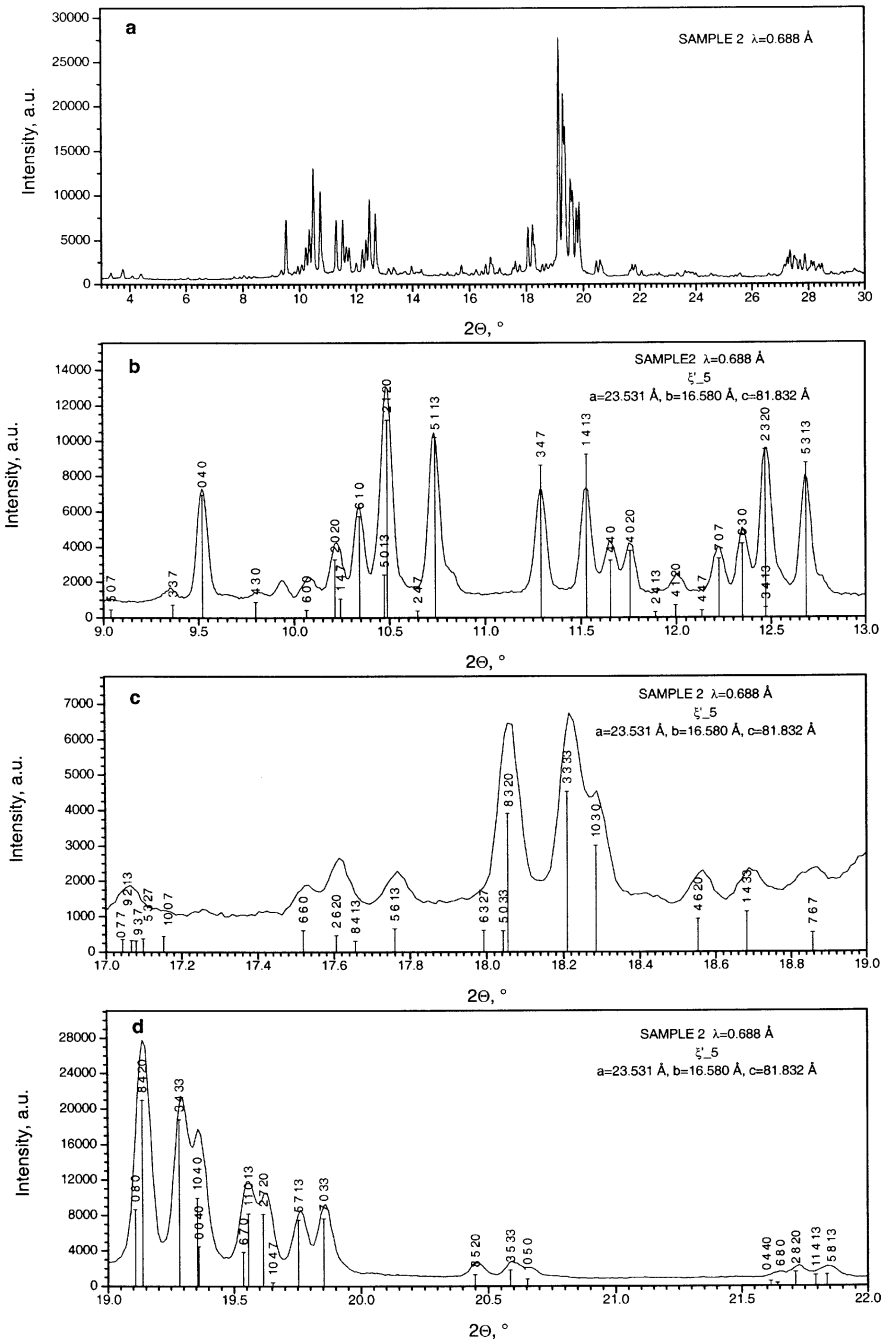

Fig. 2. X-ray powder diffraction pattern ($\theta - 2\theta$ scan, $\lambda = 0.688$ Å) of sample 2. $\theta - 2\theta$ scan is measured with a θ step equal to 0.005°. The lines drawn are lines connecting data points. (a) The whole spectrum. The indexed spectrum in the following regions: (b) $9° < \theta < 13°$, (c) $17° < \theta < 19°$ and (d) $19° < \theta < 22°$. The weak peak which appears at $2\theta = 9.935°$ can be attributed to the (0 1 20) reflection (calculated $2\theta = 9.936°$). It is not reported in (b) because it is arising from the (0 1 3) reflection of the ξ' structure (intensity = 0.004 I_1).

(Figs. 3b–d). It is therefore easy to understand why indexing such diffraction patterns is not a simple routine operation.

Because the intensity of measured peaks in the ξ'_3 and ξ'_5 states are in close qualitative relation with the peak intensities calculated from the ξ' structure, it is tempting to describe the ξ'_5 and ξ'_3 states as "perturbed" states of the ξ' structure. The structural perturbation is one-dimensional, lies along the c direction and is coherent over large distances (the width of diffraction peaks being as the same experimental resolution).

It is interesting to note that the very weak calculated peaks ($h\,k\,l$): $h+\ell = 2n+1$ seem to be absent of the diffraction patterns. In order to learn more about this structural

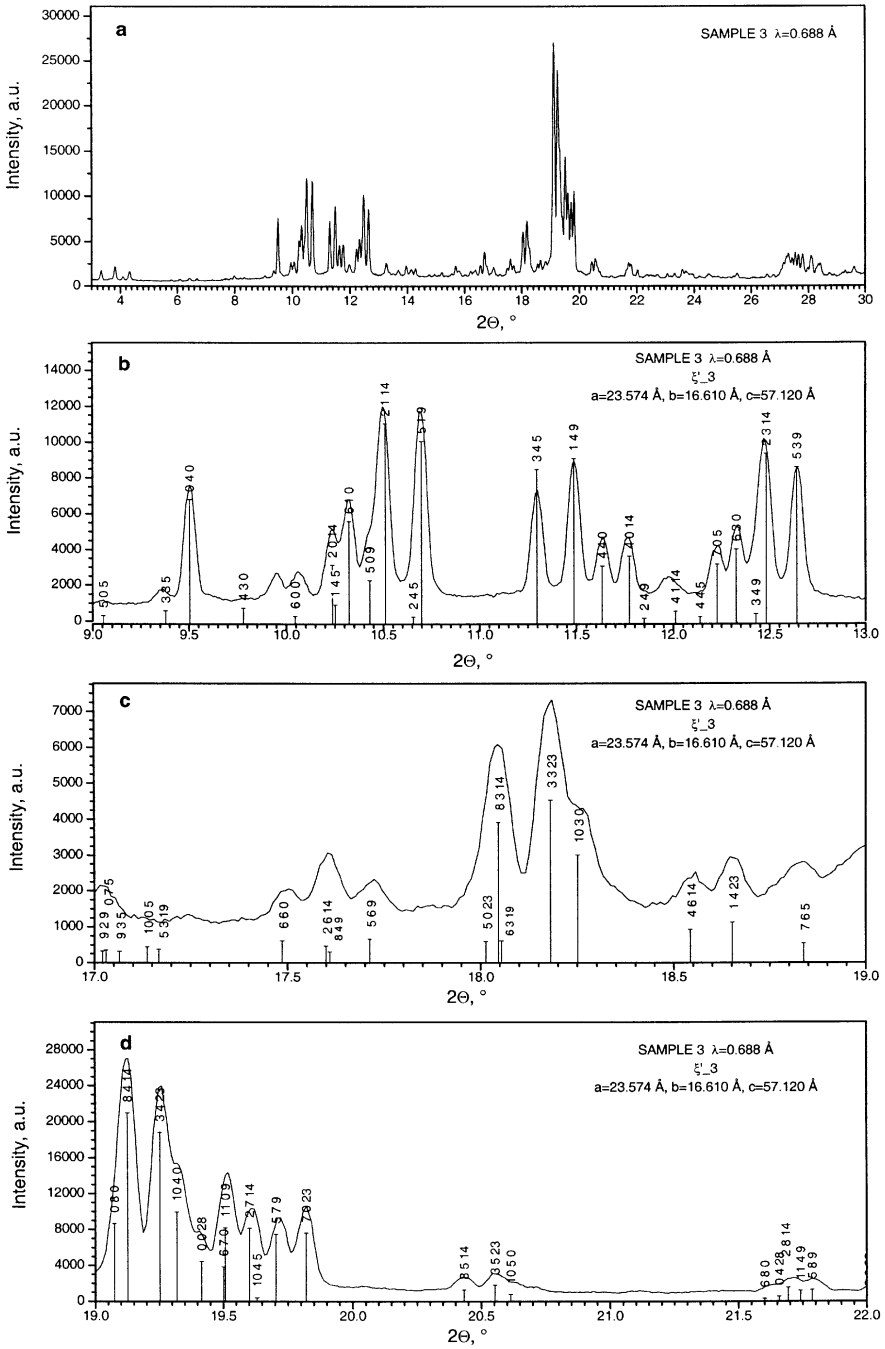

Fig. 3. X-ray powder diffraction pattern ($\theta - 2\theta$ scan, $\theta = 0.688$ Å) of sample 3. $\theta - 2\theta$ scan is measured with a θ step equal to 0.005°. The lines drawn are lines connecting data points: (a) The whole spectrum. The indexed spectrum in the following regions: (b) $9° < \theta < 13°$, (c) $17° < \theta < 19°$ and (d) $19° < \theta < 22°$. The weak peak which appears at $2\theta = 9.95°$ can be attributed to the (0 1 14) reflection (calculated $2\theta = 9.961°$). It is not reported in (b) because it is arising from the (0 1 3) reflection of the ξ' structure (intensity = 0.004 I_1).

"perturbation", we decided to perform X-ray diffraction experiments on single crystals.

3.2 X-ray single crystal diffraction study

A thin platelet (0.15 mm × 3 mm × 3 mm) was cut off from the K1 sample. Monochromatic X-ray precession diffraction patterns were obtained (Laboratoire de Physique des Solides, Orsay, France) for different orientations of the platelet. The incident wavelenght $\lambda = 1.542$ Å (CuKα) was selected using the (0 0 2) reflection of a pyrolytic graphite monochromator.

A series of precession films giving the patterns of reciprocal planes containing $(0\,k\,\ell)$, $(1\,k\,\ell)$, $(2\,k\,\ell)$, $(h\,0\,\ell)$

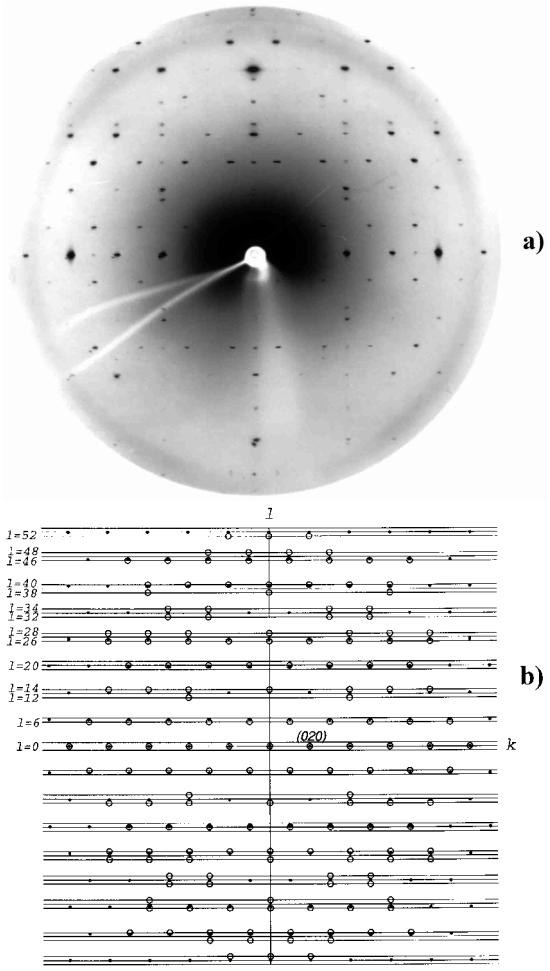

Fig. 4. (a) Monochromatic X-ray precession diffraction pattern of the K1 sample showing the equatorial reciprocal plane (1 0 0). (b) Analysis of the diffraction pattern – open circles give the positions of all observed $(0\,k\,\ell)$ diffraction peaks, the lattice parameters $b = 16.700 \pm 0.030$ Å and $c = 82.61 \pm 0.37$ Å $= c_{\xi'}(5+\tau)$ allow indexing all peaks, – for comparison black dots give the calculated diffraction peak positions of the ξ' structure (the lattice parameters $b = 16.700$ Å and $c = 12.482$ Å are used in the calculation). The series of straight lines allows to easily deduce the selection rules of the ξ'_5 structure. Note that the observed peaks of ξ'_5 are all very close to the calculated peaks of the ξ' structure. Due to the long exposure time, note the presence of few very weak peaks with half integer indices due to the presence in the X-ray incident beam of a very slight contamination by $\lambda/2$.

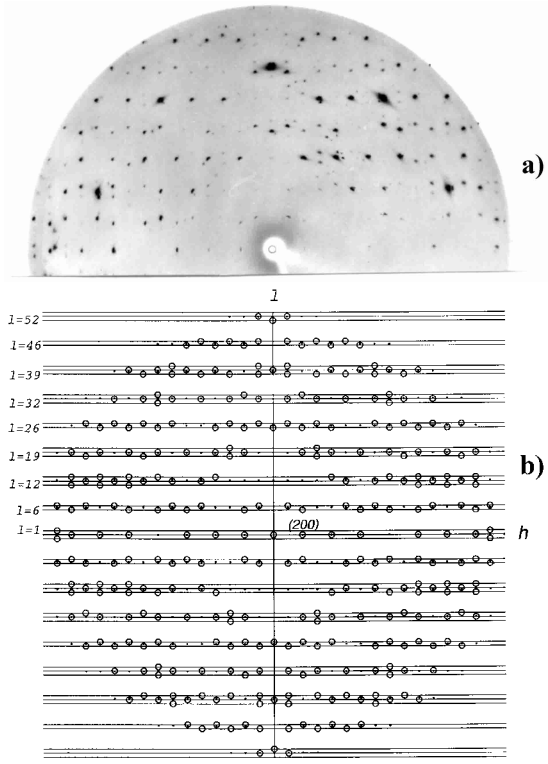

Fig. 5. (a) Monochromatic X-ray precession diffraction pattern of the K1 sample showing the equatorial reciprocal plane (0 1 0). (b) Analysis of the diffraction pattern – open circles give the positions of all observed $(h\,0\,\ell)$ diffraction peaks, the lattice parameters $a = 23.547 \pm 0.050$ Å and $c = 82.61 \pm 0.37$ Å $= c_{\xi'}(5+\tau)$ allow indexing all peaks, – for comparison black dots give the calculated diffraction peak positions of the ξ' structure (the lattice parameters $a = 23.547$ Å and $c = 12.482$ Å are used in the calculation). The series of straight lines allows to easily deduce the selection rules of the ξ'_5 structure. Note that the observed peaks of ξ'_5 are all very close to the calculated peaks of the ξ' structure. Note that the additional peaks are due to a slight contamination by a very small crystallite.

and $(h\,k\,0)$ reflections have been taken. Figures 4a, 5a, 6a show the results obtained for the three equatorial reciprocal planes (1 0 0), (0 1 0) and (0 0 1). Positions of all the observed diffraction peaks (hollow circles) are given in Figures 4b, 5b and 6b. All the diffraction peaks can be indexed with the following orthorhombic cell parameters:

$$a = 23.547 \pm 0.050 \text{ Å}, \; b = 16.700 \pm 0.030 \text{ Å}, \; c = 82.61 \pm 0.37 \text{ Å}.$$

The reflections $(0\,k\,\ell)$ and $(h\,0\,\ell)$ are located on the layers $\ell = 0, 6, 12, 14, 20, 26, 28, 32, 34, 38, 40, 52$ and $\ell = 0, 1, 6, 7, 12, 13, 14, 19, 20, 21, 26, 27, 32, 33, 34, 39, 40, 41, 46, 47, 52, 53$ respectively and the reflection conditions are as follows:

$$(0kl),\ l = 2n$$
$$(h0l),\ h + l = 2n.$$

The $(h\,k\,0)$ reflections conditions are identical to the reflection conditions observed in the ξ' structure, *i.e.*:

$$(hk0),\ h = 2n$$
$$(h00),\ h = 2n$$
$$(0k0),\ k = 2n.$$

The black dots in Figures 4b, 5b, 6b indicate the positions that the selective reflections of the ξ' structure should

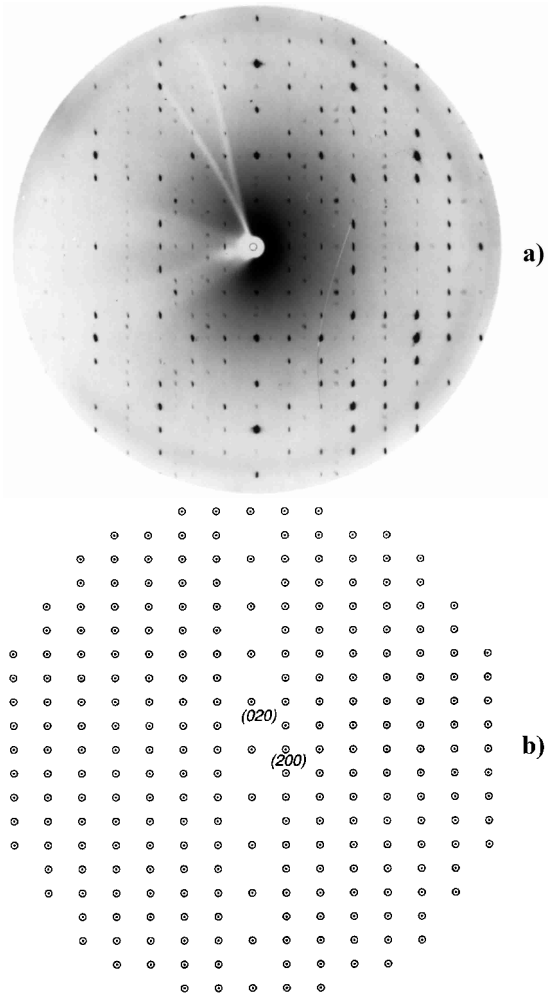

Fig. 6. Monochromatic X-ray precession diffraction pattern of the K1 sample showing the equatorial reciprocal plane (0 0 1). (b) Analysis of the diffraction pattern – open circles give the positions of all observed $(hk0)$ diffraction peaks, the lattice parameters $a = 23.547 \pm 0.050$ Å and $b = 16.700 \pm 0.030$ Å allow indexing all peaks, – the open circles coincide with the calculated diffraction peak positions of the ξ' structure (black dots). Due to the long exposure time, note the presence in (a) of very weak peaks with half integer indices due to the presence in the X-ray incident beam of a very slight contamination by $\lambda/2$. This harmonic arises from the monochromatisation of the beam using the (0 0 2) reflection of pyrolytic graphite. We have checked that all these peaks were excited by $\lambda/2$. It is the reason why, they are not shown in (b).

have. In these simulations we have used the cell parameters deduced from our precession patterns: $a_{\xi'} = 23.547$ Å, $b_{\xi'} = 16.700$ Å, $c_{\xi'} = 82.61/(5+\tau)$ Å for the lattice parameters of the ξ' structure. As it can be seen from these figures, the measured diffraction peaks $(0\,k\,\ell)$ and $(h\,0\,\ell)$ (hollow circles) are located on layers taking integer values l on both sides of layers of black dots. This means once more that the structure of the ξ'_5 state is different from the structure of the ξ' phase, but not too much.

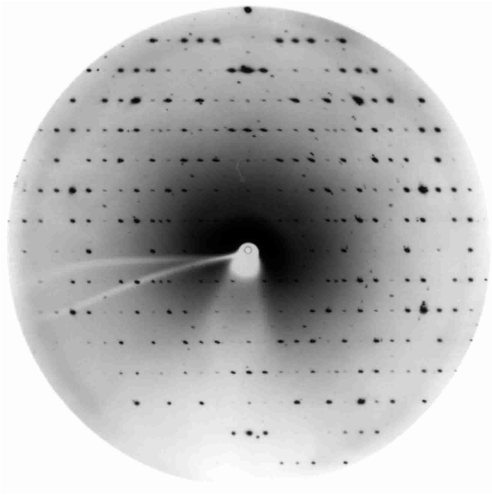

Fig. 7. Monochromatic X-ray precession diffraction pattern of the K2 sample showing the equatorial reciprocal plane (0 0 1) of the ξ' structure. Due to the long exposure time, note the presence of very weak peaks with half integer indices due to the presence in the X-ray incident beam of a very slight contamination by $\lambda/2$.

From the precession films giving the patterns of reciprocal planes containing the $(1\,k\,\ell)$, $(2\,k\,\ell)$ reflections, an additional reflection condition

$$(hk\ell),\ h + \ell = 2n$$

can be deduced. This confirms the absence of these diffraction peaks in powder diffraction patterns. The resulting orthorhombic space group obeying all these selection rules is the $B22_12$ space group. This space group is equivalent to the space group with the standard symbol $C222_1$ of International Tables of Crystallography *via* a basis transformation interchanging **b** and **c**.

A similar study has been performed on a platelet extracted from the K2 single grain. A series of precession films giving the patterns of reciprocal planes containing $(h\,0\,\ell)$, $(h\,1\,\ell)$, $(h\,2\,\ell)$ and $(0\,k\,\ell)$ reflections has been taken. In this sample, all the diffraction peaks can be interpreted as arising from the ξ' structure with lattice parameters $a_{\xi'} = 23.543 \pm 0.050$ Å, $b_{\xi'} = 16.643 \pm 0.05$ Å, $c_{\xi'} = 12.374 \pm 0.040$ Å and space group Pnma (or $P2_1ma$). The symmetry and lattice parameters of the ξ' structure of [5,8] being confirmed, the description of the ξ' phase in terms of icosahedral quasicrystal approximant cannot be appropriate.

Figure 7 shows the diffraction pattern of the equatorial reciprocal plane (0 1 0). No traces of the ξ'_5 state can be detected in this platelet taken from the bulk of the K2 single grain, contrary to the powder taken from the surface of the extremity of the sample 2.

These results show that the sample 2 which was believed to be a single crystal of ξ' phase (at the beginning of these studies), in fact contains several single grains and at least two states, ξ' and ξ'_5, and that the greatest care must be taken in measuring physical properties on such big grains.

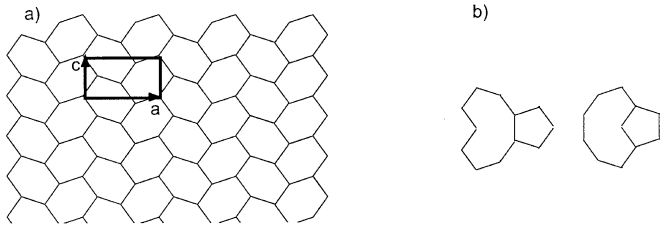

Fig. 8. (a) Schematic representation of the ξ' structure in the (**a**, **c**) plane. (b) The two kinds of "defects" frequently observed in HREM images.

4 Discussion: A geometrical model for the ξ'_n states

The experimental Fourier space obtained by several techniques (X-ray powder diffraction, X-ray precession, electron diffraction [22]) reveals the existence of several states in close relation with the ξ' phase. The ξ'_3 and the ξ'_5 states have been observed in this study.

High-resolution electron microscopy experiments along the b direction indicate that the ξ' phase contains "defects" [8]. We show in Figure 8a a tiling of squashed hexagons as the ξ' structure appears in the (**a**, **c**) plane of HREM images. This tiling is obtained in joining centres of decagonal columns. The periodicity along the column is equal to the $b_{\xi'}$ lattice parameter and the edge length of hexagons is equal to $c_{\xi'}/\tau$. Figure 8b shows the two kinds of cluster "defects" (pentagon + nine-edge polygon) observed in this phase and as they were described by Klein [8,9] from their HREM study.

Figure 9a shows how the parameter $c = c_{\xi'}(1+\tau)$ can be obtained from a periodic tiling of these "defects". This tiling only contains pentagons and nine-edge polygons.

Figure 9b shows how a periodic tiling with the lattice parameter $c = c_{\xi'}(2+\tau)$ can be obtained. This tiling was observed in the so-called ξ' phase in small regions of HREM image [8]. It is worth noting that we were able also to recognize such a tiling in small regions of HREM image taken by Sun and Hiraga [21] in the $Al_{75}Pd_{20}Mn_5$ alloy. It seems that there exists only one manner to obtain a tiling with this lattice parameter. This does not remain true for the states ξ'_n with $n \geq 3$ where the number of different tilings is increasing with n. In the $n = 3$ and $n = 5$ states, we should have to choose, among all the different possible tilings, the tiling possessing the symmetry elements of the space group deduced from our diffraction study, in particular the base B of the orthorhombic cell has to be centred. Among all the tilings, obtained in mixing layers of squashed hexagons and layers of "defects", only one is found obeying this condition, both for the $n = 3$ and $n = 5$ states. Figures 9c and 9d show these geometrical models. One can see that the number of layers of squashed hexagons is increasing with n whereas the number of layers of "defects" remains constant and equal to 2, $\forall n$. These structures can be described as periodic arrangements of "defect" structures along the c direction, the "defect" density being decreasing with n increasing. With n increasing, the layers of "defects" separating "antiphase domains" of ξ' structure can be regarded as a kind of "antiphase domain boundaries".

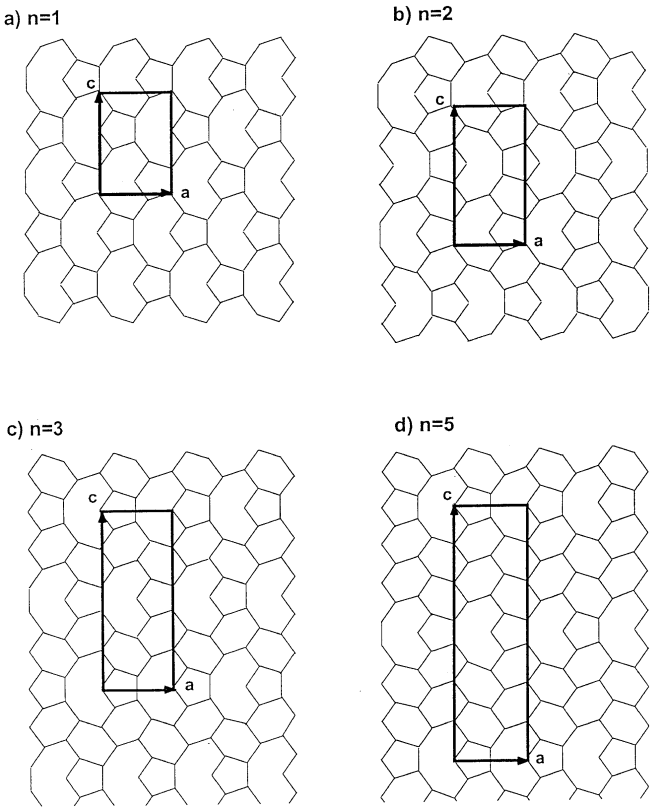

Fig. 9. Periodic tilings with the following lattice parameters: (a) $a_{\xi'}$ and $c_{\xi'}(1+\tau)$, (b) $a_{\xi'}$ and $c_{\xi'}(2+\tau)$, (c) $a_{\xi'}$ and $c_{\xi'}(3+\tau)$, (d) $a_{\xi'}$ and $c_{\xi'}(5+\tau)$.

5 Summary and concluding remarks

The starting point of this work was the difficulty to describe the orthorhombic ξ' structure as a rational approximant structure derived from the 6D Al-Pd-Mn icosahedral quasicrystal structure by applying a uniform shear to its perpendicular space.

A complete Fourier space study, by means of X-ray diffraction has:

- firstly confirmed symmetry and lattice parameters of the ξ' phase, definitively putting an end to the discussion about the ξ' phase in terms of an approximant of the Al-Pd-Mn icosahedral quasicrystalline phase;
- and secondly revealed complex structures in close relation with the ξ' structure.

These complex structures with long range order have been described as resulting from a periodic "perturbation" of the ξ' structure along the c direction. This perturbation with periodicities $c_{\xi'}(3+\tau)$ and $c_{\xi'}(5+\tau)$ have been observed in this study and structural models based on periodic arrangements of "defects" layers separating layers of ξ' phase have been proposed. They take into account the symmetry deduced from X-ray diffraction patterns.

These complex structures certainly correspond to intermediate states between the ξ' phase and the decagonal phase with 16 Å periodicity. By joining centres of decagonal atom clusters observed in HREM images taken with the incident beam parallel to the tenfold axis in the rapidly solidified decagonal quasicrystal $Al_{75}Pd_{20}Mn_5$ alloy, Sun and Hiraga [21] have obtained a tiling containing decagons, pentagons, squashed hexagons and nine-edge polygons. By analysing their results in the perpendicular space they shows that their observed tiling arise from a quasiperiodic structure containing "random phason strain or linear phason strain". Among these four kinds of polygons, only three are needed to describe the tilings of intermediate phases and only one is present in the ξ' phase.

Looking in details at the electron diffraction pattern obtained by Sun and Hiraga [21] on the as-cast $Al_{75}Pd_{20}Mn_5$ alloy, we were able to index it using the lattice parameters of the ξ'_2 structure. Sun and Hiraga point out that the same kind of diffraction patterns was also frequently observed in samples annealed to 720 °C and 800 °C. This lets suppose that this "faulted" ξ' phase (ξ'_2) is stable at high temperature. It would be interesting to determine the temperature and composition domains where the ξ', ξ'_2, ξ'_3 and ξ'_5 structures could be observed.

A last concluding remark is the observation of an important diffuse background in our powder diffraction patterns (Figs. 1a, 2a, 3a) allowing us to conclude that significant disorder coexists with long range order in the ξ'_3 and the ξ'_5 structures. At the present time the nature of disorder is not known. Diffuse scattering was observed and interpreted in icosahedral quasicrystals [23–25], decagonal quasicrystals [26] and complex Frank-Kasper phases [27].

We acknowledge P. Bastie, B. Grushko and M. Laridjani for useful discussions. We also acknowledge M. Feurbacher for providing us the samples.

References

1. L. Ma, R. Wang, K.H. Kuo, Scripta Metallurgica **22**, 1791 (1988)
2. Y. Matsuo, K. Hiraga, Phil. Mag. Lett. **70**, 155 (1994)
3. K. Hiraga, E. Abe, Y. Matsuo, Phil. Mag. Lett. **70**, 163 (1994)
4. A-P. Tsai, Y. Yokoyama, A. Inoue, T. Masumoto, J. Mater. Res. **6**, 2646 (1991)
5. M. Boudard, H. Klein, M. de Boissieu, M. Audier, H. Vincent, Phil. Mag. A **74**, 939 (1996)
6. B. Grushko, private communication
7. I.R. Fisher, M.J. Kramer, Z. Islam, T.A. Wiener, A. Kracher, A.R. Ross, T.A. Lograsso, A.I. Goldman, P.C. Canfield, Mat. Sci. Eng. **294-296**, 10 (2000)
8. H. Klein, Ph.D. thesis INPG, Grenoble (1997)
9. H. Klein, M. Audier, M. Boudard, M. de Boissieu, L. Beraha, M. Duneau, Phil. Mag A **73**, 309 (1996)
10. M.V. Jaric, S. Y. Qiu, *Quasicrystals 12th Taniguchi Symposium*, edited by T. Fujiwara, T. Ogawa (Springer-Verlag, Berlin, 1990), pp. 48–56
11. T. Janssen, Europhys. Lett. **14**, 131 (1991)
12. D. Gratias, A. Katz, M. Quiquandon, J. Phys. Cond. Matt. **7**, 9101 (1995)
13. M. Quiquandon, A. Katz, F. Puyraimond, D. Gratias, Acta Cryst. A **55**, 975 (1999)
14. M. Quiquandon, A. Quivy, J. Devaud, F. Faudot, S. Lefebvre, M. Bessiere, Y. Calvayrac, J. Phys. Cond. Matt. **8**, 2487 (1996)
15. M. Audier, M. Duneau, M. Vacher, *Adv. Phys. Metall., Sel. Pap. Proc. Int. Conf. (1996), Meeting Date 1994, pp. 61–72*
16. F.J. Edler, M.A. Estermann, T. Haibach, W. Steurer, *Aperiodic'97, Proceedings Int. Conf. Aperiodic Cryst. (1998), Meeting Date 1997, pp. 155–159*
17. H. Zhang, K.H. Kuo, Phys. Rev. B **41**, 3482 (1990)
18. F. Dénoyer, *From quasicrystals to more complex systems*, edited by F. Axel, F. Dénoyer, J.P. Gazeau (EDP Sciences Springer-Verlag, Berlin, Heidelberg), pp. 23–48
19. L. Beraha, M. Duneau, H. Klein, M. Audier, Phil. Mag. A **76**, 587 (1997)
20. N. Shramchenko, F. Dénoyer, in preparation
21. W. Sun, K. Hiraga, Phil. Mag. A **73**, 951 (1996)
22. M. Yurechko, B. Grushko, private communication
23. M. Laridjani, J. Phys. I France **6**, 1347 (1996)
24. P. Donnadieu, F. Dénoyer, J. Phys. I France **6**, 1477 (1996)
25. N. Schramchenko, H. Klein, R. Caudron R. Bellissent, Mat. Sci. Eng. **294-296**, 335 (2000) and N. Schramchenko, Ph.D. thesis, Paris 7 (2001)
26. F. Frey, Mat. Sci. Eng. **294-296**, 178 (2000)
27. M. Laridjani, P. Donnadieu, F. Dénoyer, Struct. Chem. **13**, 387 (2002)